Counter-current gas-liquid flow in vertical narrow channels. Film characteristics and flooding phenomena

E.I.P. Drosos, S.V. Paras and A.J. Karabelas
Department of Chemical Engineering and
Chemical Process Engineering Research Institute
Aristotle University of Thessaloniki
Univ. Box 455, GR 54 124 Thessaloniki, GREECE

Abstract: Flooding experiments have been carried out in a vertical rectangular channel with 10 mm gap between its parallel plates, using smooth inlet and outlet conditions, with air and two liquids (i.e. water and water/butanol solution). The critical gas velocity, U_G, at the onset of flooding tends to decrease with increasing liquid feed rate, as expected. There is a Re_L range (~150-250), for both liquids, where the critical velocity is weakly dependent on the liquid Reynolds number, and the incipient flooding mechanism involves wave growth and instability including breakage of wave crests. At Re_L>250 a stronger dependence of U_G on Re_L is observed, attributed to a different flooding mechanism, i.e. "bridging" of growing waves due to the relatively narrow gap. Concerning fluid properties, differences are observed (compared to water) in the flooding velocities with the lower interfacial tension butanol solution. Experimental data on liquid film characteristics with counter-current gas flow have also been obtained to facilitate data interpretation. Film thickness power spectra provide evidence that by increasing air flow the wave structure is significantly affected; e.g. the dominant wave frequency is drastically reduced.

Keywords: Gas-liquid flow, counter-current, narrow vertical channel, flooding, film characteristics.

Introduction

In counter-current gas-liquid flow, the onset of flooding is identified by the critical gas rate at which partial liquid flow reversal is observed. The phenomenon of flooding is of considerable technological importance being a limiting factor in the operation of various types of two-phase equipment including the common reflux condensers. The purpose of this work is to study flooding in a vertical uniform rectangular channel with relatively small gap. Such a channel is considered to simulate in a simplified manner, a single flow "element" of a compact condenser.

The amount of work on counter-current flow in *vertical rectangular channels* is limited, particularly for a narrow gap between the plates (Bankoff et al., 1986). Biage (1989) conducted flooding tests in a vertical channel with porous liquid inlet and outlet sections and a relative large channel gap (25mm). Osakabe & Kawasaki (1989) carried out "top flooding" experiments in thin rectangular passages (i.e. 10x100, 5x100 and 2x100mm) motivated by problems in the nuclear industry. Larson et al. (1994) reported experiments with similar liquid feeding conditions, in *very narrow* rectangular channels of 1.1 and 2.2mm gap. Zapke & Kroeger (2000) studied the effect on flooding of the duct geometry (with duct height and width 50 to 150mm and 10 to 20mm, respectively) and of fluid properties, using water, methanol, propanol and several gas phases. They concluded that the flooding gas velocity, U_G, is strongly dependent on the duct height, the phase densities and duct inclination; furthermore U_G tends to decrease with increasing liquid viscosity, which seems to have a stronger effect than the surface tension. Vlachos et al. (2001) reported flooding data obtained in a vertical rectangular channel with 5 and 10mm gap between its main flat parallel plates.

Experimental set-up and procedure

An experimental facility was specifically built to study counter-current gas-liquid flow and flooding (***Figure 1***). Two-phase flow is developed in a 70cm high and 12cm wide rectangular channel made of Plexiglas. The spacing between the two parallel plates is 10mm. The air entrance section is constructed with special care to achieve well-developed conditions before air contacts the falling liquid film. Liquid phase is introduced at the top and removed from the bottom via porous sections (covering the entire active channel width), embedded flash with the main flat surfaces. The length of the test section, measured between the bottom edge of the inlet porous wall and the top edge of the outlet porous section, is 38cm. A small amount of gas flows out together with the liquid film, removed in the lower porous wall section, which is measured by a rotame-

ter after separating the two fluids. On top of the measuring section there is a phase separator from which the liquid phase is fed back to the storage tank, whereas air is released to the atmosphere.

Experiments were carried out under adiabatic flow conditions with water and a water/butanol solution (2.5%) at ambient temperature (~20°C) (***Table 1***) and slightly elevated pressure (up to 1.1 bar absolute) maintained inside the test section to facilitate liquid removal through the outlet porous wall section. Before each set of experiments the inner surface of the Plexiglas test section was treated with a silica sol in order to improve its wettability. Each experiment was carried out by pre-pressurizing the

Table 1. Properties of liquids used in the experiments.

	water	***2.5% butanol***
μ, $kg\ m^{-1}s^{-1}$	0.00102	0.00098
ρ, $kg\ m^{-3}$	1000	992
σ, $kg\ s^{-2}$	0.075	0.040
contact angle, *deg*	50 (25)*	30 (10)*

*on treated surface

channel with the gas flowing at a relatively low rate. Then, the required liquid flow rate was fixed and the liquid flowed steadily down to the outlet porous wall section where it exited the channel. Next, the gas flow rate was progressively increased stepwise until the onset of flooding. *The latter is defined as the condition where at least part of the liquid flow is reversed in direction and carried above the liquid entrance section.* Visual studies were made using a *Redlake MotionScope PCI*® high-speed camera, either slightly above the liquid exit or below the liquid entrance section. Film thickness was also measured, using the "parallel-wire conductance" technique, in order to determine the liquid film characteristics.

Results

Visual Observations - Critical Flooding Velocities

From visual observations and high-speed camera recordings, the following mechanisms are identified at the onset of flooding. At low Re_L (<250), the mechanism involves roughly 2-D "isolated" waves, covering part of the liquid film surface in the lateral direction, that tend to grow and be swept up the channel due to drag and pressure forces exerted by the gas flow. Furthermore, liquid droplets torn off the surface waves are entrained by the gas upflow. At higher Re_L (>250) some waves on the liquid film surface tend to become unstable with their amplitude rapidly increasing till they partially block the gap (*"local bridging"*). The liquid of these waves is then forced by the gas to move upwards.

The observed critical flooding velocities U_G, for the two different liquids used are plotted in ***Figure 2.*** Here Re_L is defined as $4\Gamma_L/\mu_L$, where Γ_L is the liquid mass flow rate per unit length of channel circumference and μ_L is the liquid viscosity. The data show

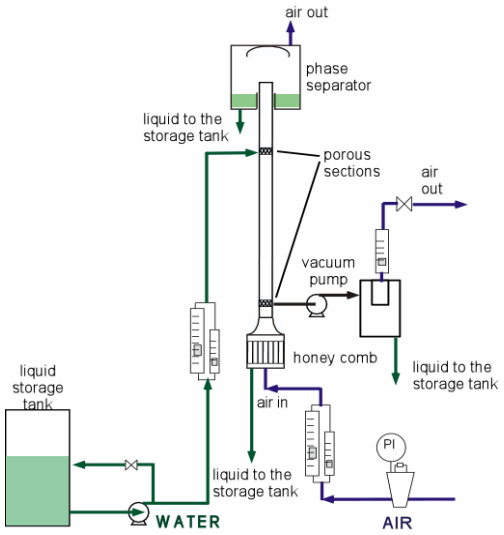

Figure 1. A schematic of the experimental set-up for studying counter-current gas-liquid flow and flooding

that at relatively low liquid flow rates, there is a significant decrease of the critical air velocity, U_G,, with Re_L. By further increasing the liquid flow rate in the range Re_L ~150-250 the flooding velocity appears to be weakly dependent on the liquid Reynolds number. This behavior may be attributed to the structure of the free falling liquid film under the action of gravity. The different mechanism ("bridging") observed for incipient flooding at high Re_L seems to be reflected in the changing slope of the data at Re_L~250. The rather strong influence of the fluid

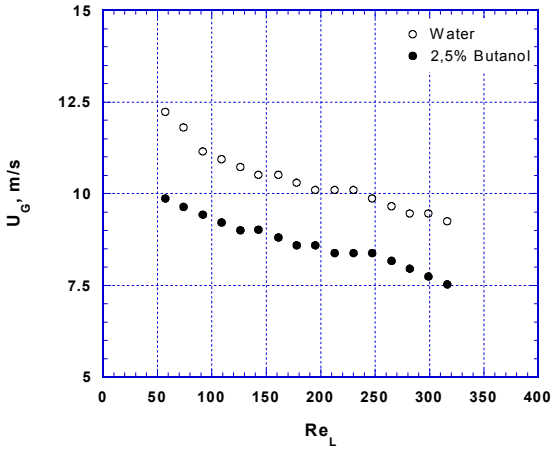

Figure 2. Superficial gas velocity plotted vs liquid *Re*, at the onset of flooding.

properties on critical flooding velocity is evident in ***Figure 2.*** With the butanol solution flooding occurs at lower air velocities compared to water, mainly because of its lower surface tension.

As is well-known, at small Re_L numbers the liquid film is very thin and laminar. The pictures in ***Figure 3*** is an example of liquid film development at Re_L=109 (near the liquid entrance) for butanol solution, at small to rather high gas flow rates (Q_G = 2.58-10.31*l*/s), but still below critical conditions. The film appears to be initially smooth and undis-

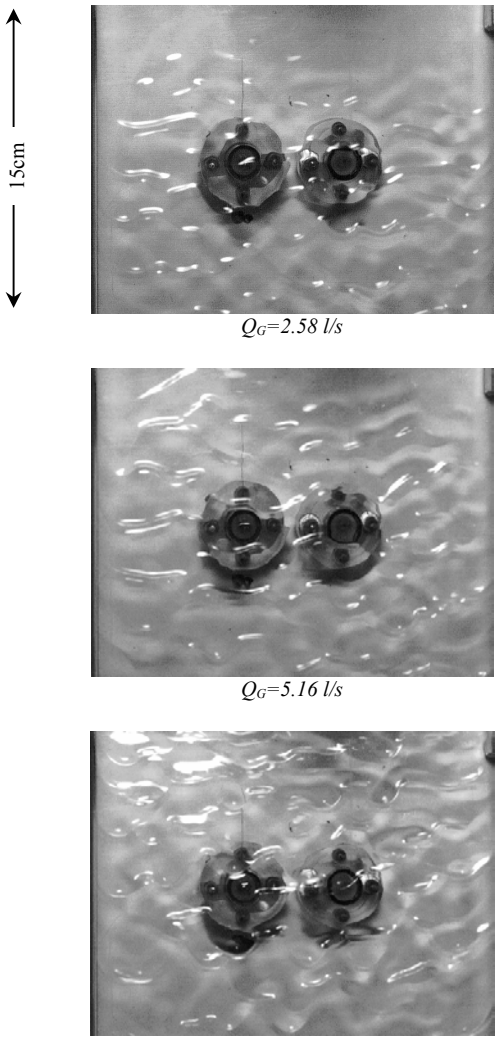

Figure 3. Liquid film flow on the channel main parallel plate, for Re_L=109 and various air flow rates.

turbed. Downstream nearly two-dimensional disturbances develop first, evolving into a three-dimensional, small-amplitude wave structure. These waves are characterized by (somewhat faster moving) pebble-like wave fronts, clearly identified in the picture. This behavior is very similar to that previously observed in free falling films in this Laboratory (Vlachos et al., 2001) and elsewhere (e.g. Pierson et al., 1977, Chang et al., 1994). By increasing the gas flow rate, the wave disturbance on the film surface moves upstream covering the entire plate surface up to the liquid entry.

Film Thickness Characteristics

Water and a water/butanol solution (2.5%) were also used for measurements of film characteristics near the bottom of the channel (36cm from liquid entrance), as incipient flooding was mainly observed close to the liquid exit. Experiments were conducted without and with counter-current air flow. In ***Figure 4*** the *mean* film thickness for the butanol solution case, during counter-current flow is plotted as a dimensionless film thickness ratio, by dividing with the mean thickness for falling film (without air). It is evident that increasing gas rate results in increasing *mean* thickness as flooding is approached. This increase is rather small at low U_G, but as the gas rate approaches the critical value for flooding, the *mean* thickness increases sharply. This trend was also observed by Zabaras (1985). Another feature of the liquid film worth examining is the value of the

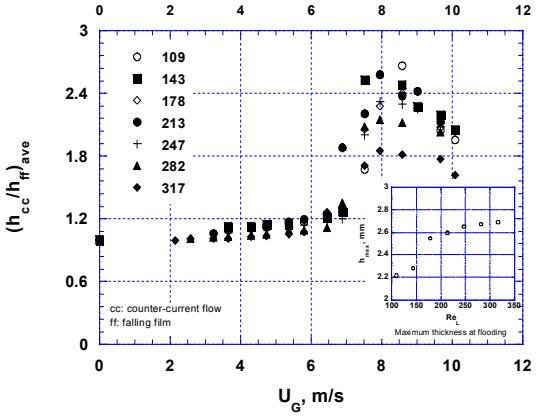

Figure 4. Ratio of mean film thickness at counter-current flow, over the free falling film thickness vs. superficial gas velocity, for various liquid *Re*.

maximum film thickness at incipient flooding. This value is estimated as the average of the ten largest values of film thickness observed in a 80sec (with a sampling rate of 125Hz) recording which corresponds to flooding and it can be seen for various Re_L, as an insert in ***Figure 4***. It is important to note that the maximum film thickness for Re_L<250 is significantly lower compared to the length of the wire probe employed (~2.7mm), whereas for Re_L>250 it is very close to this length. Therefore, the true mean film thickness at flooding point for Re_L>250, may be larger than one can measure with the present probes.

The sharp increase of the *RMS* values of film thickness at flooding, shown in ***Figure 5*** provides additional evidence of the change of the wave structure. Comparing ***Figures 4*** and ***5***, it appears that by increasing the gas flow rate above critical conditions, the mean and *RMS* values tend to decrease due

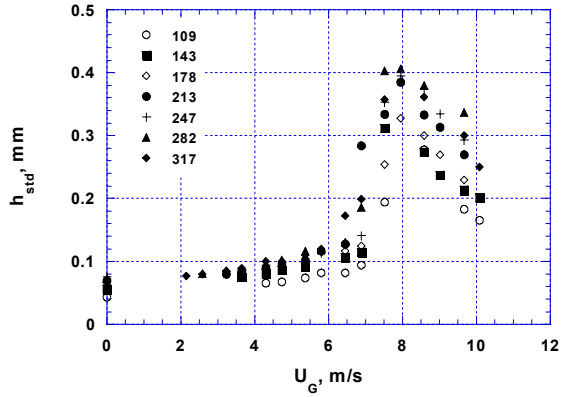

Figure 5. *RMS* values of film thickness at countercurrent flow vs superficial gas velocity, for various liquid *Re*.

to the decreasing downflow rate at the location of the channel were characteristics of liquid film are examined (bottom edge).

Typical *power spectral density (PSD)* of the liquid film thickness fluctuations at the bottom edge of the channel are presented in ***Figures 6*** and ***7***, for the case of the butanol solution and for two different values of Reynolds number. A very pronounced maximum, at frequencies between 7 and 10Hz is observed for the *free falling film*, for both Reynolds numbers and it can be related to the periodic passage of the waves covering the liquid surface. This dominant frequency tends to increase with increasing Re_L, as expected. The dominant frequency decreases with increasing air velocity to a value approximately 1-3Hz at flooding and beyond i.e. when liquid flow reversal occurs at this point (bottom edge) of the channel. The reduction of the dominant frequency is another manifestation of the drastic liquid film restructuring due to counter-current gas flow, at conditions near flooding. Growth of mean film thickness and reduced liquid wave celerity are also observed under the same conditions. Another interesting feature of the spectral density functions in ***Figures 6*** and ***7*** is the apparent increase of the energy conveyed by the waves, with increasing air flow rate.

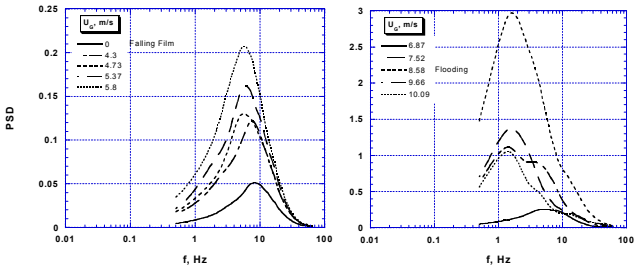

Figure 6. Power spectral density function of film thickness at counter-current flow, for Re_L=109 and for various gas velocities.

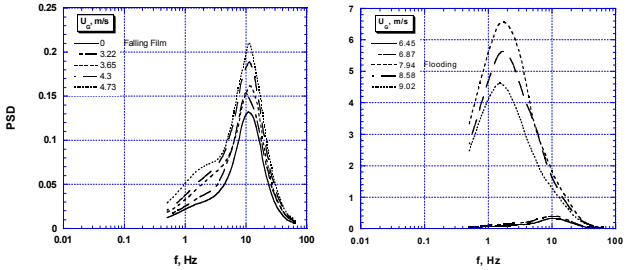

Figure 7. Power spectral density function of film thickness at counter-current flow, for Re_L=247 and for various gas velocities.

Concluding Remarks

The observations suggest that the dominant mechanism of flooding at the smaller values of Reynolds numbers examined, involves growth and flow reversal of nearly 2-D isolated waves covering part of the liquid film surface in the lateral direction, with liquid droplets torn off the wave surfaces entrained by the gas. At higher Re_L (>250), local bridging of surface waves is the dominant mechanism. The gap size appears to influence the characteristic Re_L at which "bridging" occurs first.

The critical gas velocities at the onset of flooding in general tend to decrease with increasing liquid rate, as expected. It is interesting that for both liquids there is a region of Re_L (150-250), where critical flooding velocity is weakly dependent on liquid flow rate. Concerning fluid properties, significant differences are observed (compared to water) in the flooding velocities with the lower interfacial tension butanol solution.

Under conditions approaching flooding, drastic changes seem to occur in liquid film flow. Interpretation of instantaneous film thickness measurements shows that a sharp increase of the mean film thickness and of RMS values take place near the onset of flooding; furthermore, a significant reduction of the dominant wave frequency is observed.

References

Bankoff, S.G. & Lee, S.C. 1986 A critical review of the flooding literature. In *Multiphase Science and Technology*, Chapter 2 (*Edited by* Hewitt, G.F., Delhaye, J.M. and Zuber, N.), pp. 95-180. Hemisphere, New York.

Biage, M. 1989 Structure de la surface libre d'un film liquide ruisselant sur une plaque plane vertical et soumis a un contre-courant de gas: Transition vers l'ecoulement cocourant ascendant. Ph.D. Thesis, Inst. Nat. Polytech. de Grenoble, France.

Larson, T.K., Oh, C.H. & Chapman, J.C. 1994 Flooding in a thin rectangular slit geometry representative of ATR fuel assembly side-plate flow channels. *Nucl. Eng. Des.* ***152***, 277-285.

Osakabe, M. & Kawasaki, Y. 1989 Top flooding in thin rectangular and annular passages. *Int. J. Multiphase Flow* ***15***, 5, 747-754.

Pierson, F.W. & Whitaker, S., 1977 Some theoretical and experimental observations of the wave structure of falling liquid films. Ind. Eng. Chem. Fundam. ***16*** , 401-408.

Vlachos, N.A., Paras, S.V., Mouza, A.A. & Karabelas, A.J. 2001 Visual observations of flooding in narrow rectangular channels. *Int. J. Multiphase Flow* ***27***, 8, 1415-1430.

Zabaras, G.J. 1985 Studies of vertical annular gas-liquid flows. Ph.D. Thesis, Univ. of Houston.

Zapke, A. & Kroeger, D.G. 2000 Counter-current gas-liquid flow in inclined and vertical ducts – I: Flow patterns, pressure drop characteristics and flooding. *Int. J. Mult. Flow,* ***26****, 1439-1455.*